Love waves from local traffic noise interferometry

M. Behm and R. Snieder, Colorado School of Mines

Surface-wave interferometry on local scale usually aims at recovering Rayleigh waves. This is because of the predominant use of vertical component geophones in exploration seismology and the fact that Rayleigh waves occur for any given subsurface structure. On the other hand, Love waves are present only in layered media and require horizontal component geophones for their observation. As they depend on shear-wave velocity structure and density only, the analysis of Love waves provides a potentially powerful supplement to Rayleigh wave inversion. Perhaps surprisingly, recent studies show that low-frequency Love waves (0.05–0.1 Hz) excited by the interaction of ocean waves with the ocean floor (the Earth's microseism) can be recovered by interferometry, and that their S/N is high compared to Rayleigh waves (Lin et al., 2008). On a regional scale, Jay et al. (2012) analyzed the ambient noise field in a volcanic region and found that Love waves with frequencies of about 0.3 Hz are observed more clearly than corresponding Rayleigh waves. In this article, we show that Love waves in the frequency band of 1.5 to 5 Hz can be obtained from local noise interferometry, and that they are of comparable S/N as Rayleigh waves. Thus they may also be used to constrain the near-surface structure.

Love waves in a nutshell

Love waves are horizontally polarized because they result from interaction of shear (SH) waves. As opposed to Rayleigh waves, Love waves exist in layered media only. For the one-layer case, the Love wave represents the superposition of multiply, critically reflected downgoing SH waves from the bottom of the layer (e.g., Stein and Wysession, 2003). The layer of a thickness H is then considered as a wave guide and the Love-wave velocity c_L is inbetween the shear-wave velocities of the layer and the half-space (Figure 1). In contrast, Rayleigh-wave velocities are always less than the layers shear-wave velocity. The dispersion relation shows that Love-wave velocities at low frequencies tend toward the half-space velocity β_2, while observations at high frequencies give the layer velocity β_1. Equation 1 relates the Love-wave velocity c_L to its frequency f, layer thickness H, layer and half-space shear-wave velocities β_1, β_2, and densities ρ_1, ρ_2:

$$\tan\left(\frac{2\cdot\pi\cdot f\cdot H}{c_L}\cdot\sqrt{\frac{c_L^2}{\beta_1^2}-1}\right)=\frac{\beta_2^2\cdot\rho_2\cdot\sqrt{1-\frac{c_L^2}{\beta_2^2}}}{\beta_1^2\cdot\rho_1\cdot\sqrt{\frac{c_L^2}{\beta_1^2}-1}} \qquad (1)$$

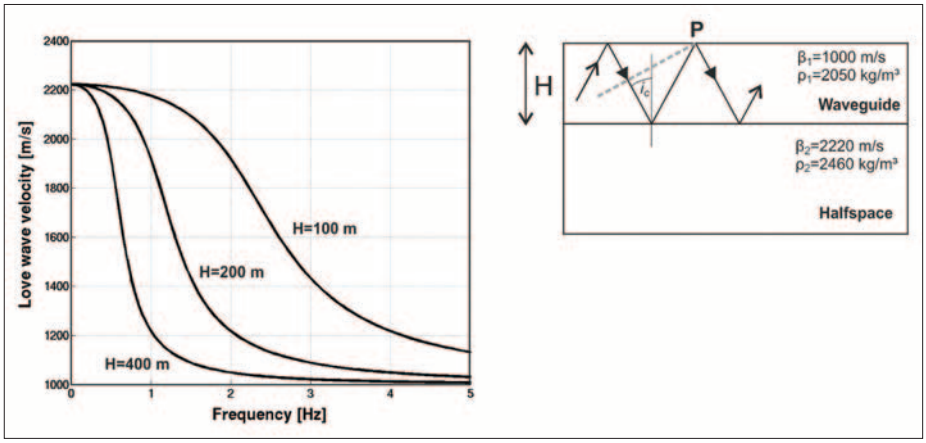

Figure 1. *Love-wave phase velocity as a function of frequency and layer thickness* H *for a layer-over-half-space model (dispersion relation).* β *and* ρ *refer to shear-wave velocity and density, and* i_c *is the critical angle. The shown raypath is not the actual raypath of the Love wave, but schematically describes critically reflected SH waves. The dashed gray line is the wavefront of the downgoing SH waves which interfere to constitute the Love wave at the surface point* P.

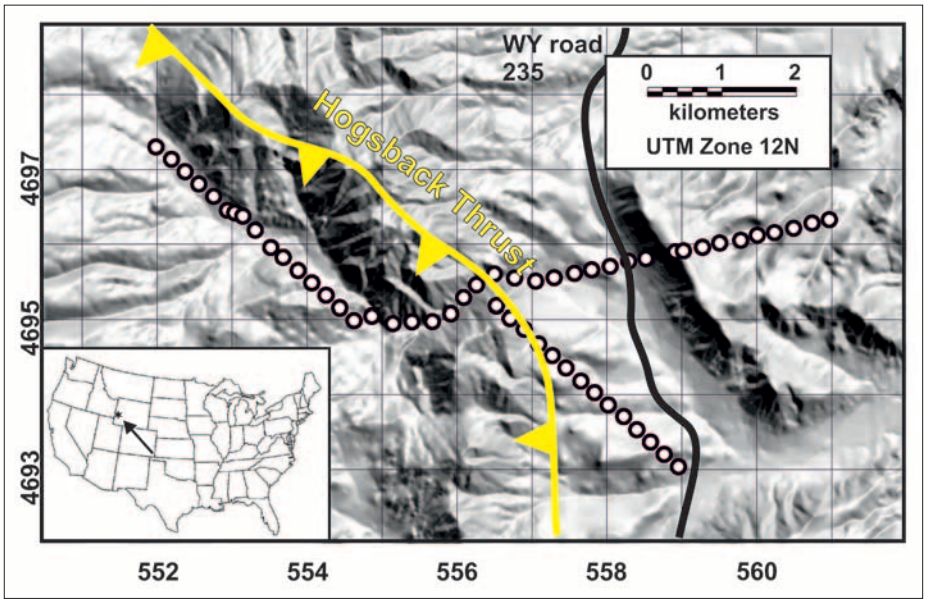

Figure 2. *The deployment of the La Barge Passive Seismic Experiment in southwestern Wyoming. White dots indicate locations of three-component instruments. The black line represents the state road contributing dominantly to the ambient noise. The Hogsback thrust is the main structural feature and separates carbonate outcrops in the west from siltstones and sandstones in the east.*

Equation 1 illustrates that, opposed to Rayleigh waves, Love-wave velocities do not depend on compressional-wave velocities. The use of Love waves thus reduces the ambiguity inherent in inversion for shear-wave structure. If the assumption of the one-layer case is well justified, the dispersion relation potentially enables us to estimate the shear-wave velocities of both the layer and the basement, and by further assuming densities, also the layer thickness. Eslick et al. (2008) examine the constraints on the subsurface settings and recording parameters for successful retrieval of Love-wave dispersion. In case of several layers, the shear-wave velocities of the layers can be determined analogously to Rayleigh waves (Xia et al., 2009). From a practical point of view, it is interesting to note that even for the one-layer case the dispersion relation is highly nonlinear and a solution for Love-wave velocity must be determined numerically. Solutions for multilayer-models and laterally varying layer thicknesses require more computational effort (e.g., Ben-Hador and Buchen, 1999). On the other hand, the nonlinearity of the dispersion relation can be employed to impose constraints on shear waves, densities, and layer thickness, provided the Love-wave velocity can be reliably observed over an appreciable frequency range.

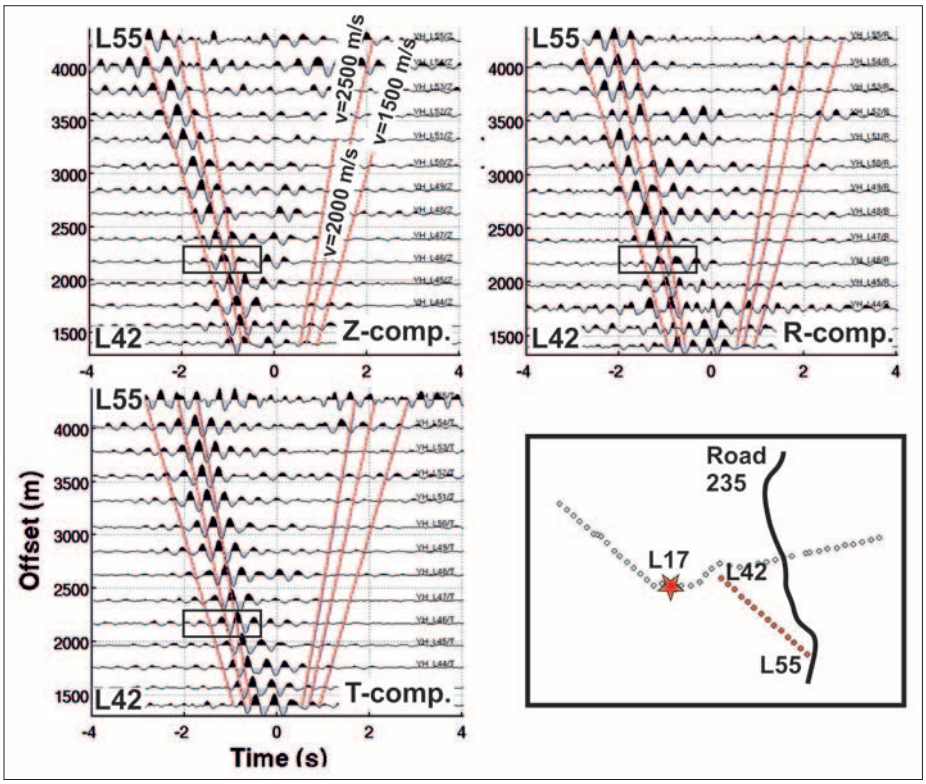

Figure 3. *Interferograms for virtual source L17 (red star) and stations L42 to L55 (red dots). The lack of causal energy results from the receiver stations being closer to the noise source (WY state road 235) than the virtual source. Dashed red lines indicate linear moveouts for velocities of 1500, 2000, and 2500 m/s. Note the higher apparent phase velocity at the transverse component (T) compared to vertical (Z) and radial (R) components. The black rectangle depicts the waveform from which the dispersion curve for raypath "A" (Figure 6) is calculated.*

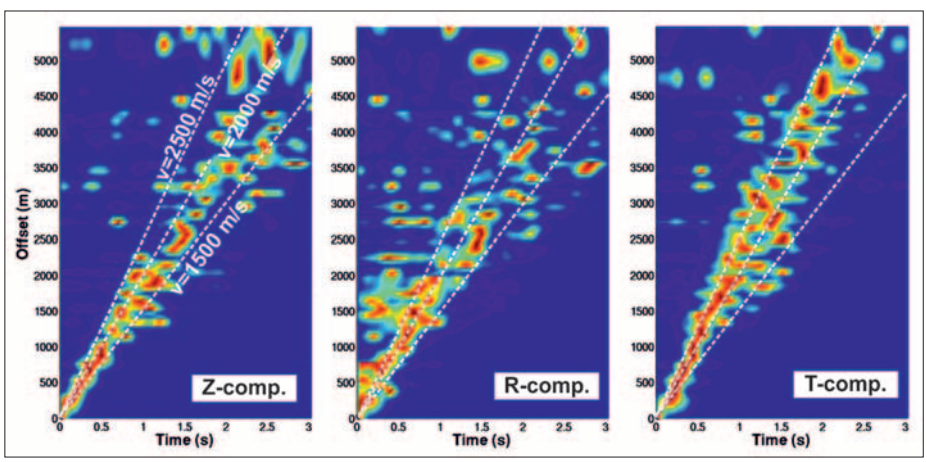

Figure 4. *Common-offset stacks of Hilbert-transformed interferograms from 530 virtual-source receiver combinations in the central part of the investigated area. Note the overall similarity of the vertical (Z) and radial (R) components, and the higher apparent group velocity of the transverse (T) component data.*

Data and interferometric processing

The La Barge Seismic Experiment is a industry-academia cooperation aiming at evaluating the feasibility of passive seismology for local subsurface characterization (Saltzer et al., 2011). From November 2008 to June 2009, 55 3C broadband stations were deployed at a spacing of 250 m in an active hydrocarbon production site in southwestern Wyoming (Figure 2). The continuous recordings and the small aperture of the array make the data set well suited for local interferometry analyses. Previous investigations (Behm et al., accepted) show that both Rayleigh- and Love-wave velocity information are obtained from traffic noise originating from a state road. We first summarize their approach and their most important findings, and then discuss the Love waves in more detail.

Each of the stations is turned into a virtual source by correlating its ambient noise recording with the ambient noise recording of every other station. It turns out that five days of continuous noise data are sufficient to recover surface waves travelling between the stations up to distances of 5 km. Analysis further shows that traffic activity from the Wyoming state road 235 in the eastern part of the deployment provides the main source

of coherent noise. The location of the road with the respect to the deployment ensures a large number of stationary phase points such that most interferograms feature clear surface-wave arrivals with high S/N. Rayleigh waves are polarized in the plane defined by the vertical and the propagation direction, and Love waves are polarized in the horizontal plane and perpendicular to the propagation direction. By rotating the horizontal components into the radial (virtual source—receiver azimuth) and transverse (90° clockwise to the azimuth) directions, it is possible to separate Love and Rayleigh waves. The slower Rayleigh wave is present on the vertical and radial components, and the faster Love wave appears on the transverse component (Figure 3). Although of overall high S/N, the interferograms are characterized by a limited bandwidth peaking at 2.5 Hz, and subsequently a sometimes ringy wavelet. The calculation of the envelope (modulus of the Hilbert-transformed interferogram) compresses oscillating wavelets and improves the delectability of the onset of the waves. It is important to note that envelope interferograms no longer represent phase velocities, but group velocities instead. All envelope interferograms from the central part of the investigated area are further stacked in offset bins (Figure 4). Although lateral velocity variations may degrade the stacks, these results also support the existence of both Rayleigh and Love waves. Vertical and radial component data appear similar with respect to apparent velocity and maximum offsets (2500–3500 m), while transverse component data feature higher apparent velocity and also more consistent arrivals at large offsets (3500–5000 m).

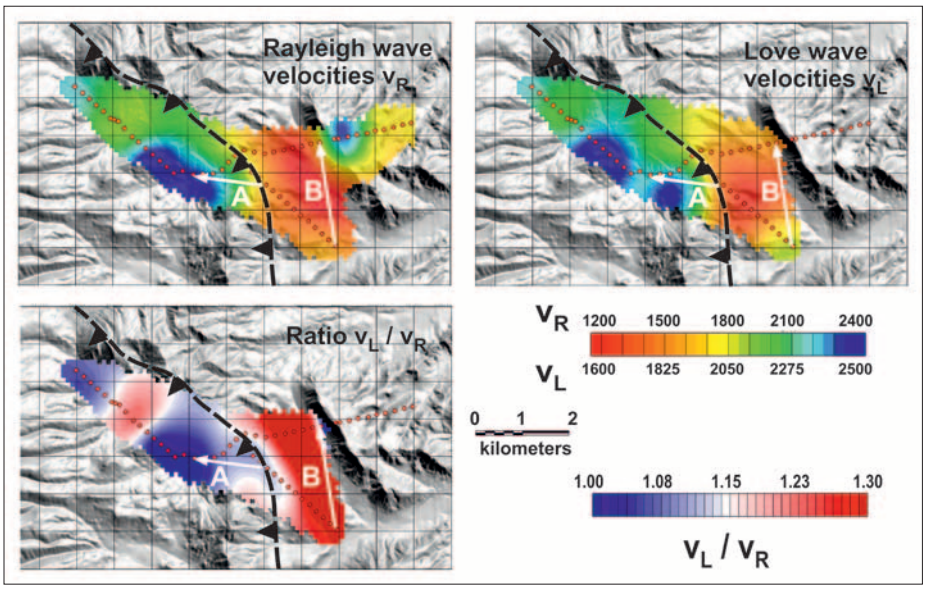

Figure 5. *Near-surface phase-velocity maps and their ratio as obtained from traveltime tomography of vertical and transverse component interferograms (from Behm et al. accepted, slightly modified). The arrows (A, B) denote the virtual source-receiver pairs for which dispersion curves are shown in Figure 6.*

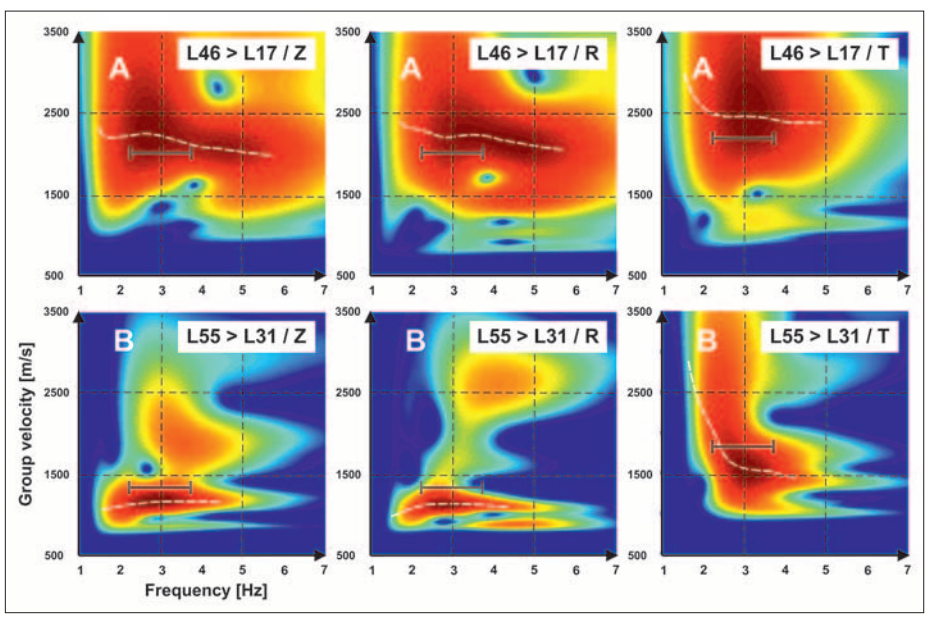

Figure 6. *Group velocity dispersion curves obtained from frequency-time analysis for two virtual source—receiver pairs (A: L46 > L17; B: L55 > L31). The white curve depicts the maximum amplitude at each frequency. Note the overall similarity of the vertical (Z) and radial (R) components, and the higher velocity and different appearance of the transverse (T) component. The gray bar shows the average phase velocity (Figure 5) along the raypath.*

Dispersion of surface waves enables us to invert for shear-wave velocity structure. In exploration seismology and near-surface investigations, the multichannel analysis of surface waves (MASW) is commonly applied to obtain Rayleigh-wave phase-velocity dispersion (Park et al., 1999). The relatively low central frequency of the obtained traffic noise interferograms in conjunction with the station spacing hampers the observation of phase velocity dispersion, while the large number of clear surface-wave arrivals allows inverting picked traveltimes for laterally varying group and phase velocities. Vertical component traveltimes provide Rayleigh-wave velocities, and transverse component traveltimes are inverted for Love-wave velocities (Figure 5). With respect to the wavelength, those velocities represent average surface-wave velocities from the upper 100–300 m. The results correlate well with the surface geology as the carbonates west of the Hogsback thrust are represented by relatively high velocities. Lateral resolution of the velocity maps

depends on ray coverage and picking accuracy, and we estimate it to range between 500–1000 m.

Group velocity dispersion of Rayleigh and Love waves

In contrast to the MASW method, the relatively sparse distribution of broadband instruments on continental scale led to methods to derive group velocity dispersion between station pairs based on the frequency-time analysis (FTAN; Dziewonski et al., 1969; Levshin et al., 1989). With this approach, the surface wave travelling between two stations is reconstructed by interferometry. The interferogram is filtered in different frequency bands, where each band is defined by a Gaussian function of a central frequency and given half-width. After filtering, the envelope of the trace is calculated. By knowing the offset between the two stations, the time axis of the trace is converted to velocity and the maximum of the envelope is picked for each central frequency. The obtained group velocity dispersion curve can then be inverted for a shear-wave velocity-depth function representing the region between the stations. If station coverage is dense, a tomographic approach for a 3D shear-wave velocity model is also feasible. This method has been applied successfully to ambient noise from globally distributed earthquakes to delineate crustal and mantle structures (e.g., see the overview given by Bensen et al., 2007). As with MASW, the inversion for shear-wave velocities assumes a layered 1D model. The evident lateral variation in the investigated area limits the general applicability of the FTAN algorithm, but nonetheless we are able to calculate group velocity dispersion curves for selected receiver pairs (Figure 6). To minimize the contribution of spurious energy, we mute the interferograms for apparent velocities larger than 4000 m/s and less than 1000 m/s prior to the dispersion analysis. The raypath "A" comprises the stations L46 (virtual source) and L17 (receiver) in the high-velocity carbonates. As virtual source and receiver are interchangeable, the actual surface wave used for the calculation of the dispersion curve is seen in the acausal part of Figure 3. In contrast, the raypath "B" connects the stations L55 (virtual source) and L31 (receiver) in the low-velocity eastern part.

Vertical and radial component dispersion curves appear similar with a gentle tendency of lower velocities toward higher frequencies, while the dispersion of the transverse component with its steep slope toward the low-frequency end resembles typical Love-wave dispersion characteristics (compare with Figure 1).

Group velocities U_G and phase velocities U_P are related by

$$U_G(f) = \frac{U_P(f)}{1 - \frac{f}{U_P} \cdot \frac{dU_P}{df}}. \quad (2)$$

For a given frequency f and realistic velocities, group velocities are less than phase velocities if the phase velocities

decrease with frequency ($dU_p/df < 0$) and vice versa. The magnitude of the difference between group and phase velocities is inversely proportional to the phase velocity and to the rate of change of phase velocity with frequency. The observations for ray path "A" qualitatively agree with this general relation of phase and group velocities in that sense that group velocities are less than phase velocities. In case of raypath "B", the group velocities surprisingly appear higher than the phase velocities. However, it is noted that raypath "B" crosses the region with the strongest lateral variation, representing the westward dipping low-angle Hogsback thrust where a gradually thickening sheet of high-velocity carbonates overthrusts low-velocity sediments. This definitely represents a challenge to the simplifications inherent to both traveltime inversion and dispersion interpretation, and also illustrates limits to surface-wave inversion.

Outlook

Our study shows that locally excited Love waves in a typical exploration environment and in the frequency range of 1.5–5 Hz are of comparable, if not higher S/N than Rayleigh waves. This frequency range does not necessitate costly broadband stations as in our test study, but can be well targeted by low-frequency geophones more commonly used in exploration seismology. With more and more industrial applications relying on three-component instruments (e.g., seismic monitoring, shear-wave retrieval), the recording and potential use of Love waves for subsurface characterization becomes feasible. In particular passive seismic deployments are well suited, as surface waves can be efficiently recovered from interferometry applied to local ambient noise. Love waves are enticing because, compared to Rayleigh waves, they do not depend on P-wave velocity and thus reduce the ambiguity in extracting shear-wave velocity structure. Near-surface shear-wave velocity inversion zones might by quickly mapped by the absence of Love waves. The complementary information of Rayleigh and Love waves provides improved assessment of seismic velocities and densities. Combined dispersion measurements of Love and Rayleigh might also be used to constrain lateral variations in Earth structure (Levshin and Ratnikova, 1984) and seismic anisotropy (Montagner and Nafaf, 1986). In case when the near surface is sufficiently described by a one-layer model, the distinct shape of the Love-wave dispersion curve could facilitate to estimate layer and half-space shear-wave velocities and densities simultaneously. TLE

References

Ben-Hador, R. and P. Buchen, 1999, Love and Rayleigh waves in non-uniform media: Geophysical Journal International, **137**, no. 2, 521–534, http://dx.doi.org/10.1046/j.1365-246X.1999.00790.x.

Bensen, G. D., M. H. Ritzwoller, M. P. Barmin, A. L. Levshin, F. Lin, M. P. Moschetti, N. M. Shapiro, and Y. Yang, 2007, Processing seismic ambient noise data to obtain reliable broad-band surface wave dispersion measurements: Geophysical Journal International, **169**, no. 3, 1239–1260, http://dx.doi.org/10.1111/j.1365-246X.2007.03374.x.

Behm, M., R. Snieder, and G. M. Leahy, Retrieval of local surface wave velocities from traffic noise—an example from the LaBarge basin (Wyoming): accepted for publication in Geophysical Prospecting.

Dziewonski A. M., S. Bloch, and M. Landisman, 1969, A technique for the analysis of transient seismic signals: Bulletin of the Seismological Society of America, **59**, 427–444.

Eslick, R., G. Tsoflias, and D. Steeples, 2008, Field investigation of Love waves in near-surface seismology: Geophysics, **73**, no. 3, G1–G6, http://dx.doi.org/10.1190/1.2901215.

Jay, J. A., M. E. Pritchard, M. E. West, D. Christensen, M. Haney, E. Minaya, M. Sunagua, S. R. McNutt, and M. Zabala, 2012, Shallow seismicity, triggered seismicity, and ambient noise tomography at the long-dormant Uturuncu volcano, Bolivia: Bulletin of Volcanology, **74**, no. 4, 817–837, http://dx.doi.org/10.1007/s00445-011-0568-7.

Levshin, A. L., and L. I. Ratnikova, 1984, Apparent anisotropy in inhomogeneous media: Geophysical Journal of the Royal Astronomical Society, **76**, no. 1, 65–69, http://dx.doi.org/10.1111/j.1365-246X.1984.tb05022.x.

Levshin, A. L., T. B. Yanovskaya, A. V. Lander, B. G. Bukchin, M. P. Barmin, L. I. Ratnikova, and E. N. Its, 1989, Seismic surface waves in a laterally inhomogeneous Earth: Norwell.

Lin, F., M. P. Moschetti, and M. H. Ritzwoller, 2008, Surface wave tomography of the western United States from ambient seismic noise: Rayleigh and Love wave phase velocity maps: Geophysical Journal International, **169**, 1239–1260.

Montagner, J. P. and H. C. Nataf, 1986, On the inversion of the azimuthal anisotropy of surface waves: Journal of Geophysical Research, **91**, B1, 511–520, http://dx.doi.org/10.1029/JB091iB01p00511.

Park, C. B., R. D. Miller, and J. Xia, 1999, Multichannel analysis of surface waves: Geophysics, **64**, no. 3, 800–808, http://dx.doi.org/10.1190/1.1444590.

Saltzer, R., G. M. Leahy, J. Schmedes, J. Roth, and E. Rumpfhuber, 2011, Earthquakes—A naturally occurring source of low frequency data: 81st Annual International Meeting, SEG, Expanded Abstracts, 3689–3693, http://dx.doi.org/10.1190/1.3627967.

Stein S. and M. Wyssesion, 2003: An introduction to seismology, earthquakes, and earth structure: Blackwell publishing.

Xia, J., R. Cakir, R. D. Miller, C. Zeng, and Y. Luo, 2009, Estimation of near-surface shear-wave velocity by inversion of Love waves: 79th Annual International Meeting, SEG, Expanded Abstracts, 1390–1394, http://dx.doi.org/10.1190/1.3255109.

Acknowledgments: This work was funded by ExxonMobil. We thank Matt Haney for reviewing the manuscript. IRIS DMC was used to access the waveform data.

Corresponding author: mbehm@mines.edu